Astronomy & Astrophysics manuscript no. Zimovets_Nakariakov_Loops_resp1_VMN_IVZ

December 17, 2014

Excitation of kink oscillations of coronal loops: statistical study

I.V. Zimovets[1,2] and V.M. Nakariakov[1,3,4,⋆]

[1] Centre for Fusion, Space and Astrophysics, Department of Physics, University of Warwick, CV4 7AL, UK

[2] Space Research Institute (IKI) of Russian Academy of Sciences, Profsoyuznaya St. 84/32, 117997 Moscow, Russia
e-mail: ivanzim@iki.rssi.ru

[3] Astronomical Observatory at Pulkovo of the Russian Academy of Sciences, 196140 St Petersburg, Russia

[4] School of Space Research, Kyung Hee University, 446-701 Yongin, Gyeonggi, Korea

December 17, 2014

ABSTRACT

Context. Solar flares are often accompanied by kink (transverse) oscillations of coronal loops. Despite intensive study of these oscillations in recent years mechanisms for their excitation remain unrevealed.

Aims. To clarify the excitation mechanisms for kink oscillations of coronal loops.

Methods. We analyse 58 kink oscillation events observed by the Atmospheric Imaging Assembly (AIA) onboard the Solar Dynamics Observatory (SDO) during its first four years (2010-2014) with the use of the *JHelioviewer*. Association of these oscillation events with flares, lower coronal ($r \lesssim 1.4R_\odot$) eruptions and plasma ejections, coronal mass ejections (CMEs) and coronal type II radio bursts is studied.

Results. **It is found that 44 out of these 58 oscillation events (76%) were associated with CMEs observed in the white light emission. Moreover, 57 events (98%) were accompanied by lower coronal eruptions/ejections (LCEs) observed in the EUV band in the parental active regions. An LCE was not clearly seen only in one event but it was definitely associated with a CME. The main observational finding is that the kink oscillations were excited by the deviation of loops from their equilibria by a nearby LCEs in 55 events (95%). In 3**

⋆Corresponding author: V. M. Nakariakov, V.Nakariakov@warwick.ac.uk

remaining events it was difficult to reliably determine the cause of the oscillations because of limitations of the observational data. We also found that 53 events (91%) were associated with flares. In five remaining events the parental active regions were behind the limb and we could not directly see flare sites. It indicates that there is a close relationship between these two kinds of the solar activity. However, the estimated speeds of a hypothetical driver of kink oscillations by flares were found to be low than 500 km/s in 80% of cases. Such low speeds are not in favour of the association of the oscillation excitation with a shock wave, as it has usually been assumed. The fact that only 23 (40%) of the oscillation events were found to be associated with coronal type II radio bursts is also against the shock wave mechanism for the excitation of kink oscillations.

Conclusions. The performed statistical analysis shows that the most probable mechanism for the excitation of kink oscillations of coronal loops is the deviation of loops from their equilibrium by nearby eruptions or plasma ejections rather than a blast shock wave ignited by a flare.

Key words. Sun: magnetic loops – Sun: oscillation – Sun: flares – Sun: eruptions – Sun: coronal mass ejections (CMEs) – shock waves

Use \titlerunning to supply a shorter title and/or \authorrunning to supply a shorter list of authors.

1. Introduction

Kink oscillations of coronal loops are one of the most debated physical phenomena in solar physics. The oscillations are usually seen as periodic harmonic displacements of the axes of loops seen in 171Å and 195Å bandpasses of coronal EUV imagers (Aschwanden et al. 1999; Nakariakov et al. 1999). **Evidences of kink oscillations of coronal loops have recently been found with the use of the radio observations (e.g., Inglis & Nakariakov 2009; Khodachenko et al. 2011; Mossessian & Fleishman 2012; Kupriyanova et al. 2013; Zaqarashvili et al. 2013).** The typical periods of the oscillations are about several minutes, and the displacement amplitude is typically several Mm (see De Moortel & Nakariakov 2012; Liu & Ofman 2014, for a recent comprehensive reviews). Kink oscillations of neighbouring loops have usually different periods, amplitudes and phases. In the majority of cases, only the fundamental spatial harmonics is observed, with the maximum of the transverse displacement near the loop top and the node of the oscillations at the footpoints. However, in several cases the second harmonics was detected too. In the vast majority of observed cases, the oscillations are seen to be of the horizontal polarisation. Kink oscillations are detected in two regimes, the high-amplitude rapidly decaying oscillations (Nakariakov et al. 1999), and the recently discovered low-amplitude decayless oscillations (Nisticò et al. 2013). In the following we concentrate on the high-amplitude rapidly decaying oscillations.

The interest in the kink oscillation is connected with its intensive use for remote diagnostics of active region plasmas (e.g. Stepanov et al. 2012). Comparison of the observed properties of kink oscillations with theoretical modelling allows for the estimation of the absolute value of the mag-

netic field in the oscillating loop (Nakariakov & Ofman 2001, e.g.), the density scale height (e.g. Andries et al. 2005), and the height variation of the loop minor radius (e.g. Verth & Erdélyi 2008). Also, the understanding of basic physical mechanisms operating in kink oscillations is important for revealing the enigmatic problem of solar and stellar coronal heating (e.g. Goossens et al. 2013).

It is commonly accepted that kink oscillations are a manifestation of the kink ($m = 1$) magneto-hydrodynamic (MHD) standing mode of a plasma cylinder (e.g. Zaitsev & Stepanov 1982; Edwin & Roberts 1983). But, there is no agreement on the physical mechanisms for their excitation. The observed timing of the appearance of kink oscillations, soon after solar flares, suggested that the oscillations were excited by a blast wave generated by a flare (e.g., Aschwanden et al. 1999; Nakariakov et al. 1999; Schrijver et al. 2002; Hudson & Warmuth 2004; Tothova et al. 2011). However, numerical simulations of this process showed that it is difficult to excite perturbations of the observed displacement amplitude of several minor radii of the loop (e.g. McLaughlin & Ofman 2008; Ofman 2009) in a loop with a low ratio of the internal to external mass densities.

There have been several alternative mechanisms proposed. The apparent proximity of some oscillating loops to topologically unstable magnetic regions, i.e. near the magnetic separatrix, led to the idea that the oscillations highlight rocking motions at the photospheric level. In this case, a small displacement of the loop footpoint is magnified by the "sensitivity" of the equilibrium magnetic topology to a small perturbation (Schrijver & Brown 2000; Schrijver et al. 2002; White et al. 2013). The apparent association of kink oscillation events with the phenomenon of coronal EUV dimming led to the development of a mechanism based on the resonant excitation of the oscillations by the aerodynamic drag force caused by periodic shedding of Alfvénic vortices (Nakariakov et al. 2009; Gruszecki et al. 2010). Another mechanism, based upon the presence of field-aligned electric currents in loops, causing their inductive interaction, was developed in Khodachenko et al. (2009). Uralov (2003) proposed that the oscillatory pattern is not an oscillation of the individual loop, but a tracer of an oscillatory wake behind a flare-generated MHD disturbance propagating across the field. Discrimination between these mechanisms requires detailed information on the relationship between the kink oscillation events and their potential drivers, such as flares, plasma ejections and eruptions.

The aim of this work is to perform a detailed study of the statistical association between events of kink oscillations and dynamical processes in the corona, that could potentially excite them. The study is based upon the utilisation of high time and spatial resolution observational data and online catalogues. The paper is organised as follows. In Section 2 we describe the data used. Section 3 contains the results obtained. Section 4 presents our conclusions.

2. Observations

2.1. Kink oscillations of coronal loops

The main object of the study is high-amplitude rapidly decaying kink oscillations of coronal loops observed in the EUV band with the Atmospheric Imaging Assembly (AIA, Lemen et al. 2012)

onboard the Solar Dynamics Observatory (SDO). The term "high-amplitude" means that the amplitude of the oscillations is at least a few minor radii of the loop, that is about the linear size of the AIA pixel, which is about $0.6''$ or 435 km at the Sun. The period of the studied oscillations is longer than a few time steps between two successive AIA images in the EUV channels, which is 12 s. Thus, our study is restricted to the analysis of loop oscillations that are well resolved with AIA and can be seen with the naked eye in a sequence of AIA images without using any special detection techniques such as the time-distant mapping or periodmapping.

Our search for kink oscillation events is restricted by the first four years of the AIA observations, i.e. by the time period from 20 May 2010 to 20 May 2014. The searching for kink oscillations was performed with the Heliophysics Events Knowledgebase (HEK; `http://www.lmsal.com/hek/`). We found 96 events marked as "Oscillation" in the HEK within the considered time interval. However, not all of them were found to satisfy the purpose of our study. First of all, we excluded from further consideration all (15) events (reported in the HEK) associated with oscillations of cold and dense filaments/prominences. Thus, 81 events were left in the preliminary list for the further analysis.

It is a very time consuming task to analyse rough AIA data for all 81 events, each lasting several tens of minutes or longer. But, this task was efficiently fulfilled with the use of the *JHelioviewer* – a visualisation tool for solar images based on the JPEG2000 compression standard (Mueller et al. 2009, `http://jhelioviewer.org/`). Its capacity is sufficient for our purposes. It allows for visualising time series of AIA images with **the average cadence of 24 s**. An important advantage of the *JHelioviewer* is the possibility to determining the solar coordinates (x, y) of each image pixel, allowing for finding the coordinates of the studied objects at the Sun at a given time.

Using the *JHelioviewer* we found that kink oscillations of coronal loops were not obvious in 37 out of 81 events in the preliminary list. Actually these 37 events were indeed accompanied by some oscillatory-like processes in the corona. However, available observational datasets did not allow us to assert with confidence that these processes were really kink oscillations of coronal loops but not some other processes such as turbulent eddies, longitudinal oscillations, complex motions of multi-loop multi-temperature structures or something else. For this reason, we excluded these events from further analysis. We also found that the AIA data were not available in the *JHelioviewer* for other 3 events from the preliminary list. Thus, only 41 out of 81 events were left in the list.

It should be noted that some of these 41 oscillatory events lasted for several hours according to the HEK. Careful consideration of such events with the *JHelioviewer* showed that they consisted of several separate events, although occurring sequentially in the same active regions. The term "separate" here means that excitation of the decaying kink oscillations in these events happened several times. Each of these sub-events we classified as a separate event. Thus, our list extended from 41 to 51 events.

Finally, we added other 7 events to the list, which were not reported in the HEK. Three of them were found by the authors of this paper (20 October 2012, 17 February 2013, 19 November

2013) and 4 of them were reported in the literature: 02 August 2010 (White & Verwichte 2012), 06 September 2011 (Verwichte et al. 2013), 08 May 2012 (White et al. 2013), and 30 May 2012 (Nisticò et al. 2013). It should be noted that White & Verwichte (2012) have also analysed an oscillatory event of 13 June 2010, which was not reported in the HEK. But the AIA data for this event was not available within the *JHelioviewer* and we did not include it in our final list.

Thus, our final list (catalogue) contains 58 events that were the clear examples of high-amplitude decaying kink oscillations of coronal loops. These events are summarised in Table 1. We should note that we did not thoroughly check all the literature on the kink oscillations detected by AIA. Therefore, it is possible that some kink oscillation events observed by AIA during the time interval of 20 May 2010 – 20 May 2014 were missing in our list. Nevertheless, we assume that the sample of 58 events is large enough to draw statistically robust conclusions about the excitation mechanisms of kink oscillations of EUV coronal loops.

Columns 1 and 2 of Table 1 contain the index number and date of each event. Column 3 contains the start times of oscillations ($t_0^{\rm osc}$). Since oscillations were detected by a naked eye, the accuracy of the determination of their start times is not high. Since in some events there were almost simultaneous oscillations of several spatially separated loops, column 3 may contain several different start times. Only start times of the most obvious (high-amplitude) loop oscillations are given. From the total set of 58 events we identified 169 different oscillating loops. Solar coordinates ($x^{\rm osc}, y^{\rm osc}$) of these oscillating loops are shown in column 4. These coordinates correspond to the part of a loop, which had the highest visible oscillation amplitude for the given loop. In most cases this corresponded to the top of the loop, indicating that, most probably, the fundamental harmonics of the kink oscillations were detected.

2.2. Flares

To check the possible solar flare activity associated with the selected loop oscillation events we used the soft X-ray reports provided by the National Oceanic and Atmospheric Administration (NOAA). These reports are provided by the National Geophysical Data Center (NGDC; `http://www.ngdc.noaa.gov/stp/space-weather/solar-data/solar-features/solar-flares/x-rays/goes/`). Columns 5 and 6 of Table 1 contain the start ($t_0^{\rm flare}$) and peak ($t_{\rm max}^{\rm flare}$) times of the associated flare X-ray emission detected in the 1-8 Å wavelength band, determined with the X-Ray Sensor (XRS) onboard the Geostationary Operational Environmental Satellites (GOES) in the studied events. Column 8 shows the X-ray class of each associated flare.

Flares were reported by the NGDC not for all studied events. For such events without reported flares we checked the original 3-second GOES data using the "GOES"package in the Solar Software (SSW). In the cases when we found an increase in the solar soft X-ray flux with respect to the background level for several consecutive data points in a half-hour vicinity of the corresponding oscillation event we added the start and peak times as well as the X-ray class of this flare event to our catalogue. Such flares (8 cases) are marked by "(ZN)"label in column 5.

It can be seen in Table 1 that 53 out of the total 58 oscillation events were surely accompanied by flares, although in the majority of cases these flares were quite weak: 10 out of 53 flares (19%) were of the B class, 25 (47%) – of the C class, 14 (26%) – of the M class, and only 4 (8%) – of the X class. In the remaining 5 events there were no obvious increases in the solar soft X-ray flux (in the GOES data) above the background level. In those events the parental active regions (and probably flares) were behind the solar limb. A look at the data obtained with the EUVI/SECCHI (Howard et al. 2008) onboard the STEREO-A and STEREO-B spacecraft revealed that all these 5 events were accompanied by some increases in the EUV brightness, localised in time and space in the corresponding active regions. This indicates that all 58 studied oscillation events were accompanied by some flaring activities related to localised releases of energy.

Column 7 of Table 1 contains solar coordinates $\left(x^{\rm flare}, y^{\rm flare}\right)$ of each detected flare. These are coordinates of the brightest pixels of the flaring site close to its geometrical centre observed in the AIA "hottest" (131 Å) channel in the vicinity of the flare X-ray peak time. These coordinates were identified using the *JHelioviewer*. In the cases when the flare site (at the photosphere) was obviously behind the east or west limb of the Sun we added "(BEL)" or "(BWL)" marks respectively to column 7.

The time difference $\Delta t^{\rm flare} = t_0^{\rm osc} - t_0^{\rm flare}$ is shown in column 9 of Table 1. It can be seen that the flares started earlier than the loop oscillations in all events except only two: N 13 and 36. This may indicate that the loop oscillations are a consequence of the flares. We estimated the speeds of a possible (hypothetical) flare driver of the oscillations in each event as a ratio of a distance between the oscillating loop and the flare site, and $\Delta t^{\rm flare}$, i.e.

$$v^{\rm flare} = \sqrt{\left(x^{\rm osc} - x^{\rm flare}\right)^2 + \left(y^{\rm osc} - y^{\rm flare}\right)^2} / \Delta t^{\rm flare}. \quad (1)$$

The speeds are shown in column 10. Figure 1 gives the histogram of $v^{\rm flare}$ values (dotted rectangles). It is seen that in the majority of cases (in 102 out of 132 cases, where it was possible to calculate $v^{\rm flare}$, i.e. in 77%) $v^{\rm flare} < 500$ km/s. Note that we restricted the horizontal axis of the histogram in Figure 1 by the value of $v^{\rm flare} = 2,000$ km/s for clarity. Anomalously high values of $v^{\rm flare}$, greater than 2,000 km/s for events N 13, 18, 48 and 52, were not included into the statistics. These values are not likely to be physically meaningful. They indicate that in this event the loop oscillations were excited by a different agent (see Section 2.3) rather than by a hypothetical wave driven by a flare.

2.3. Eruptions and plasma ejections in the lower corona

Due to continuous observations of the Sun's hemisphere that is visible from the Earth with the SDO/AIA simultaneously in different channels covering broad range of plasma temperatures, we have a good opportunity to carefully examine the presence or absence of eruptions and/or plasma ejections in the lower corona ($r \lesssim 1.4 R_\odot$) co-existing with the studied loop oscillation events. This information may help us to identify a relationship between eruptions/ejections and excitation of

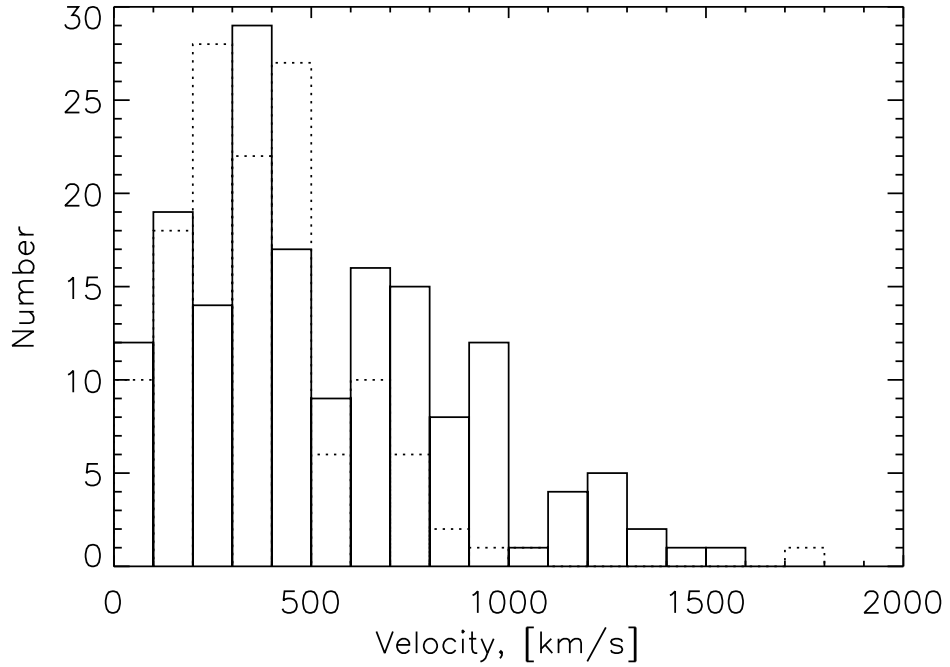

Fig. 1. Distributions of the speeds required for hypothetical agents exciting kink oscillations of coronal loops to reach the oscillation sites from the **starting point of the** lower coronal eruptions/ejections ($v^{\rm LCE}$, solid line) and **the location of the** flares ($v^{\rm flare}$, dotted lines).

kink oscillations. By the eruption we mean a sudden destabilisation and ejection of some plasma configuration in the active region of interest. It can be a cold and dense filament, a flux rope, a system of magnetic loops (a loop arcade or a more complex structure) or something else. By the plasma ejection we mean an ejection of plasmoids or jets from the flaring site along magnetic flux tubes (no matter, closed or open) of the active region.

Using the *JHelioviewer* we found that 57 out of the total 58 studied kink oscillation events (except event N 55), i.e. 98% of cases, were accompanied by evident lower coronal eruptions/ejections (LCEs) from the parental active regions. The start times ($t_0^{\rm LCE}$) of each detected LCE and solar coordinates of its initial appearance ($x^{\rm LCE}, y^{\rm LCE}$) are given respectively in columns 11 and 12 of Table 1. We should note here that event N 55 was behind the solar limb and was not accompanied by an obvious increase in the soft X-ray flux, i.e. by a flare visible from the Earth's orbit with GOES/XRS. Nevertheless, it was accompanied by a coronal mass ejection (CME, see Section 2.4). Consequently, this event should also be taken as being accompanied by an eruption/ejection in the lower corona, but it was not obviously seen with the AIA/SDO by some reason. One of the possibility is that it was a faint eruption. Analysis of the white-light CME observations with the LASCO/SOHO (Brueckner et al. 1995) in this event confirms this simple interpretation. Thus, it can be concluded that all studied kink oscillation events were accompanied by LCEs in the corresponding parental active regions. This fact is of crucial importance for understanding the excitation mechanisms of coronal loop oscillations (see the discussion below).

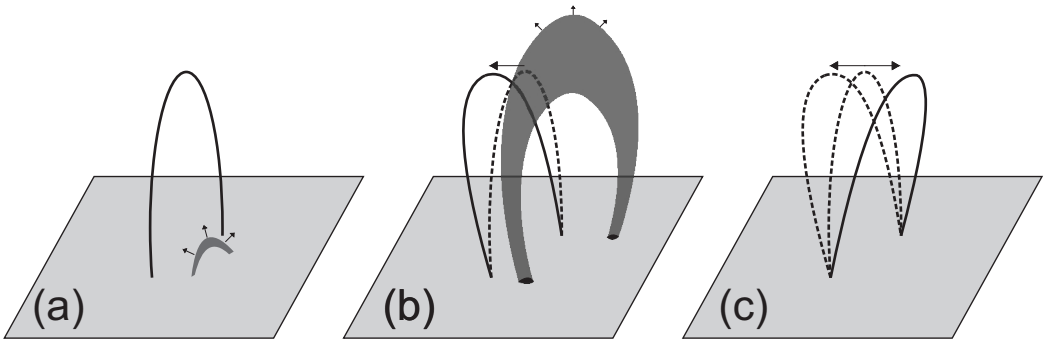

Fig. 2. Schematic illustration of the mechanism for the excitation of kink oscillations of coronal loops, observed in the majority of the studied events. (a) Pre-eruption state of the active region. (b) Displacement of a coronal loop (solid black curve) from its equilibrium state (dashed black line) by an erupting and expanding plasma structure, e.g. a flux rope (grey loop-shaped structure). (c) Oscillatory relaxation of the loop to its equilibrium state after the eruption.

All the observed LCEs started several tens or hundreds of seconds before the loop oscillations. The time differences between the start times of the oscillations and LCEs, $\Delta t^{\mathrm{LCE}} = t_0^{\mathrm{osc}} - t_0^{\mathrm{LCE}}$, is given in column 13 of Table 1. As in the case of the flares, the positive values of Δt^{LCE} evidence that excitation of the loop oscillations can be related to the LCEs. **The time lag between the LCEs' starting times t_0^{LCE} and the onset of the oscillation corresponds to the LCE development time from its initial location $\left(x^{\mathrm{LCE}}, y^{\mathrm{LCE}}\right)$ till its contact with the loops.**

Due to the high time cadence, sensitivity and multi-wavelength (thus, multi-temperature) character of the SDO/AIA observations it was possible to observe in details the impact (influence) of the LCEs to the nearby plasma structures, in particular, to coronal loops in each event (except event N 55 mentioned above and event N 2, see below). **Careful analysis** of the sequences of the AIA images (movies) in different channels within the *JHelioviewer* showed that in almost all events the excitation of kink oscillations was caused by the displacement of the loops from their equilibrium state, made by a nearby LCEs, and subsequent oscillatory relaxation of the loops to the pre-eruption equilibrium or to a new equilibrium state. ***This is the main result of the entire work.***

Schematic illustration of the most common situation observed is sketched in Figure 2. We marked this situation as type 1 in column 18 of Table 1. It was observed in 50 out of 58 events (86% of cases). For these cases it was found that coronal loops of the active region were in their equilibrium state before the flare and/or eruption (Fig. 2(a)). During the eruption an erupting plasma structure, i.e. a magnetic flux rope or a subsystem of unstable loops, interacts with some (but not necessarily all) coronal loops of the active region by ram and/or magnetic pressure, causing the loops to deviate from their equilibrium state (Fig. 2(b)). In other words, the loops are mechanically pushed away from the equilibrium by the moving plasma structure. After the erupting object has left the interaction region and reached greater heights in the corona the disturbed loops relax to the pre-eruption or a new state of equilibrium (Fig. 2(c)). Because of the inertia, the loops overshoot the equilibrium, and the kink oscillation occurs. The efficiency of this effect depends probably on how rapidly the displacing forces cease, in comparison with the period of the kink oscillation. Obviously, the proposed illustration is very schematic and should be considered only as a cartoon.

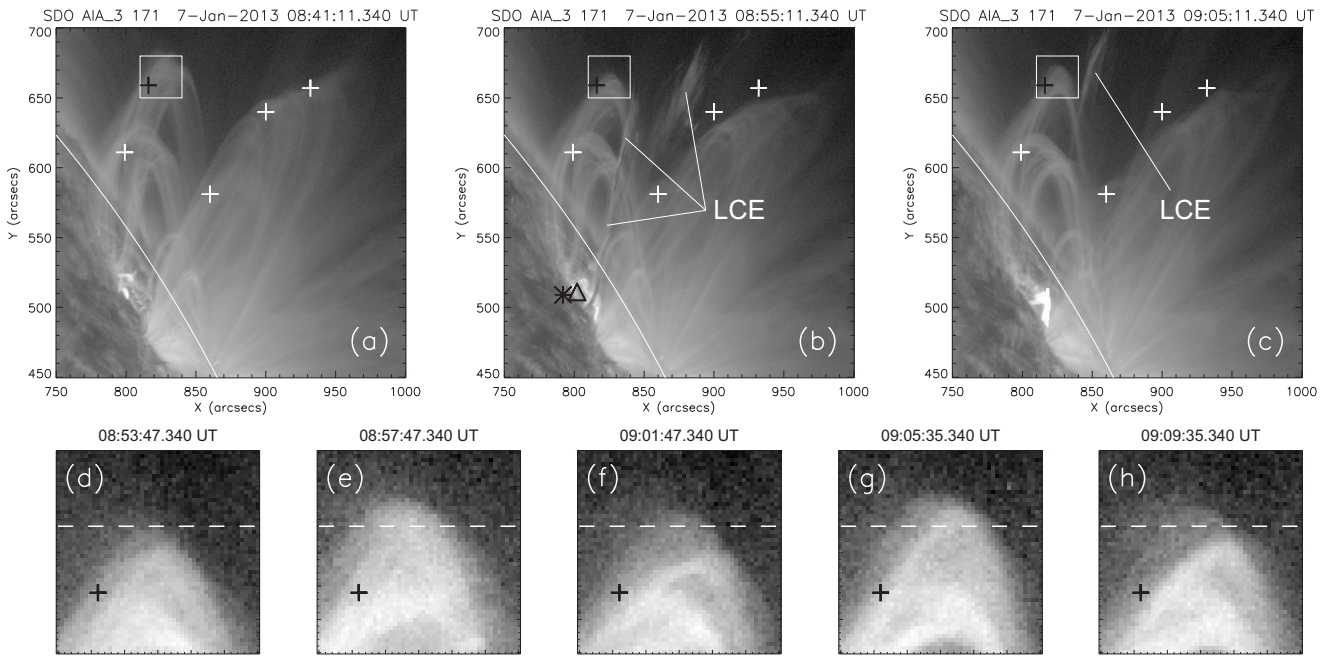

Fig. 3. Sequence of AIA 171 Å images taken during event N 44. Crosses indicate positions of the oscillating loops found with *JHelioviewer* and shown in column 4 of Table 1. The black asterisk and triangle indicate positions of the flare and the starting point of the LCE, given in columns 7 and 12 of Table 1, respectively. The white square boxes in the upper images show the region that is zoomed in the lower raw of panels. The solar limb is shown by the thin white curve. Solar coordinates of the black cross in all images are the same. The dashed horizontal line is an arbitrary reference level that aims to highlight the oscillatory behaviour of the loops.

The studied active regions had a broader variety of plasma configurations. In a more thorough study, specific details of the active region and LCE geometries should be taken into account. In particular, the LCE can interact simultaneously with several loops situated at different angles with respect to the LCE axes of symmetry.

As an example of this mechanism, we show a sequence of images taken with AIA at 171 Å during event N 44. Fig. 3(a) shows the pre-event state of the active region, which is situated close to the west limb. The active region consisted of a set of several loops of different sizes and inclined at different angles to the vertical. Fig. 3(b) shows the active region at the moment when a flux-rope-like LCE was clearly visible. This LCE propagated upward in the region between the loops and pushed them away from their equilibria in the transverse direction. The flare position and the LCE starting point close to the solar surface, found with the *JHelioviewer* (see Table 1), are indicated in the figure. Fig. 3(c) shows the instant of time when the LCE was already at some distance from the loops. The lower row of images (Fig. 3(d-h)) represents dynamics of the top of one particular loop bundle shown in the upper rows of images by the white square box. The oscillatory dynamics of the loop-top is clearly seen. Only two periods of oscillations are shown for clarity.

We also found that in 6 events kink oscillations of loops were excited in a somewhat different way. We marked these events as type 2 in column 18 of Table 1. **In these events the LCEs are also clearly seen, but it is not clear how exactly the loops become displaced. The mechanism for the excitation of kink oscillations in those cases requires a detailed dedicated study, but it**

is definitely connected with an LCE. It should be noted here that White et al. (2013) proposed another excitation mechanism for the kink oscillations observed in event N 29. We mentioned this possibility by adding the "type 3" mark into column 18 of Table 1. This event occurred far from the limb and the projection effect should be taken into account. Also the AIA images of this event were saturated by high fluxes of the EUV emission from the flare kernel. These factors strongly complicated revealing the processes operating in this active region. Both interpretations should not be excluded for this event.

In event **N** 2 the observations do not allow us to state unambiguously whether the mechanism for the excitation of the oscillation was connected with the interaction of loops with an LCE. Despite the fact that this event was undoubtedly accompanied by an LCE, as well as by a CME (see Section 2.4), direct interaction of loops with this LCE was not evident from the AIA images. This could be due to the projection effect or because of the low brightness of the LCE. However, apparently the loop oscillations in this event were excited by the interaction of the loops with the flanks of an expanding LCE (close to its bases), the apex of which was already at a high altitude (thus, it was not well seen by the AIA) during the interaction. See also the paper by Aschwanden & Schrijver (2011) where this event was studied in detail, and some other possible mechanisms for the excitation of the loop oscillations were discussed.

Since we found that the main physical agent (driver) which excited oscillations of coronal loops was an LCE we can roughly estimate its speed for each event as

$$v^{\mathrm{LCE}} = \sqrt{\left(x^{\mathrm{osc}} - x^{\mathrm{LCE}}\right)^2 + \left(y^{\mathrm{osc}} - y^{\mathrm{LCE}}\right)^2}/\Delta t^{\mathrm{LCE}}. \quad (2)$$

The values of v^{LCE} are given in column 15 of Table 1. Figure 1 gives the histogram (solid line) of the v^{LCE} values. It can be seen that, in general, values of v^{LCE} are comparable with the values of v^{flare} and are low than 500 km/s in 91 out of 165 cases, i.e. for 55% of the oscillating loops. However, the high-speed tail in the histograms is more pronounced for v^{LCE} than for v^{flare}. Further we will compare the distributions of v^{LCE} values for events with and without CMEs and for events with and without type II radio bursts.

2.4. Coronal Mass Ejections (CMEs)

We used two sources of information to check whether the studied oscillation events were accompanied by CMEs or not. The first one is the SOHO/LASCO CME catalogue (Gopalswamy et al. 2009, `http://cdaw.gsfc.nasa.gov/CME_list/`). The second one is the CACTus CME list (Robbrecht & Berghmans 2004; Robbrecht et al. 2009, `http://sidc.oma.be/cactus/`). The main difference between these two sources is that the SOHO/LASCO CME catalogue contains the CMEs manually defined from the SOHO/LASCO (Brueckner et al. 1995) data, while the CACTus CME list contains the CMEs detected with a special automatic technique from both the SOHO/LASCO and STEREO/SECCHI/COR2 (Howard et al. 2008) data. The simultaneous use of these two cata-

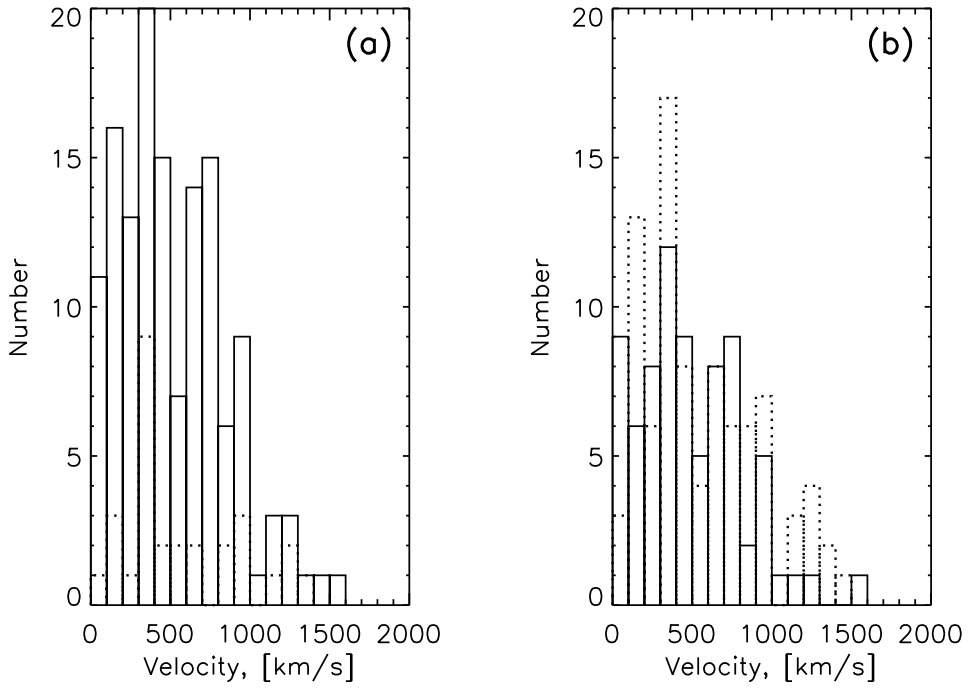

Fig. 4. Distributions of the speeds required for the excitation of kink oscillations by lower coronal eruptions/ejections, v^{LCE}, in the events: (a) with (solid line) and without (dotted line) CMEs, (b) with (solid line) and without (dotted line) coronal type II radio bursts.

logues allows for the more reliable identification of the presence/absence of CMEs in the studied events.

We consider a loop oscillation event to be accompanied by a CME if: 1) a CME was observed within one and a half hour interval after the start time of the first loop oscillation, and 2) the central position angle of the oscillating loops (measured counterclockwise from the north pole of the Sun) was in the range $\left[PA^{\mathrm{CME}} - \alpha/2, PA^{\mathrm{CME}} + \alpha/2\right]$, where PA^{CME} is the central position angle of the CME and α is its angular width measured with the SOHO/LASCO observations. The second criterion was omitted when we considered the STEREO/COR1 observations. As the first step we checked reports in the SOHO/LASCO CME catalogue. If a CME satisfying the two criteria mentioned above was in this catalogue, we marked the time of its first appearance, (t_0^{CME}, measured with an accuracy of one minute) in column 15 of Table 1. If there was no report in the SOHO/LASCO CME catalogue, we checked in the CACTus list of the CMEs detected with the SOHO/LASCO observations. If we found an appropriate CME there, we added its t_0^{CME} to column 15, labelling it with the "(C/L)" mark. If we did not find an appropriate report, we further checked for the CACTus list of the CMEs detected with the STEREO/COR2 data. In the positive identification case, we added the appropriate t_0^{CME} to column 15, labelling it with the "(C/SA)" or "(C/SB)" marks, depending on which spacecraft – respectively the STEREO-A or STEREO-B – detected the CME.

We found that 44 out of total 58 loop oscillation events (76%) were accompanied by a CME. This means that the statistical association of loop oscillation events with the CMEs is slightly worse

than with the LCEs. This is not surprising, since some of the LCEs were confined (failed) CMEs, i.e. they did not reach the heights in the corona ($r \approx 2R_{\odot}$) where they could be identified as a CME in the white light emission with the coronagraphic observations. We checked whether there was some difference between the speeds ($v^{\rm LCE}$) estimated for the LCE-induced agents possibly exciting the oscillations, in the events with and without CMEs. Distributions of $v^{\rm LCE}$ for both these types of events are shown in Figure 4(a). One can see that there is no obvious difference between the distributions of $v^{\rm LCE}$ in these two types of events, except that the statistics of the events without CMEs is three times poorer than of the events with CMEs. This indicates that the ability of an LCE to become a CME does not depend strongly on its average speed. Indeed, there are multiple evidences that the major factor determining whether an LCE will be confined (failed) or full (will become a CME), is the character of an overlying magnetic field decrease with height (e.g., Török & Kliem 2005, 2007; Liu 2008; Guo et al. 2010). Another possibility is that the estimated values of $v^{\rm LCE}$ do not give an accurate representation of the real speeds of the studied LCEs. This could be because of our estimates do not consider possible acceleration/deceleration of the LCEs during the studied time intervals. The lack of the significant difference between the $v^{\rm LCE}$-distributions in the events with and without coronal type-II radio bursts (Figure 4(b) and Section 2.5) confirms that our estimations of $v^{\rm LCE}$ are not very precise.

2.5. Coronal type II radio bursts

To find out whether the studied loop oscillation events were associated with large-scale shock waves in the corona, we checked the presence of coronal (decimetric, metric, decametric) type-II radio bursts in each case. For the first look, for each oscillation event in Table 1, we used the daily reports of the solar and geophysical activity produced by the Space Weather Prediction Center (SWPC) of the NOAA (`http://www.swpc.noaa.gov/ftpmenu/warehouse.html`) and also the monthly reports of the solar radio events detected with the Culgoora and Learmonth Radiospectrographs (`http://www.ips.gov.au/World_Data_Centre/1/9`). After this first step we checked the original radio spectrograms obtained with radio telescopes from around the globe, which performed observations of the Sun in a one-hour vicinity of each oscillation event. Radio spectrograms from the Radio Solar Telescope Network (`http://www.ngdc.noaa.gov/stp/space-weather/solar-data/solar-features/solar-radio/rstn-spectral/`) and the e-Callisto International Network of Solar Radio Spectrometers (`http://www.e-callisto.org/`) were mainly used.

The start times ($t_0^{\rm t2rdb}$) of the found type-II radio bursts and their starting frequencies ($f_0^{\rm t2rdb}$) are shown in columns 16 and 17 of Table 1 with an accuracy of 1 minute and 10 MHz, respectively. Symbol "$*$" before the starting frequencies of some type-II bursts means that the starting frequencies of these bursts were most probably higher than the given values, but radio spectrograms for the higher frequency range were not available for these events. We found that only 23 out of the total 58 loop oscillation events (40%) were associated with coronal type-II bursts. This ratio is similar to

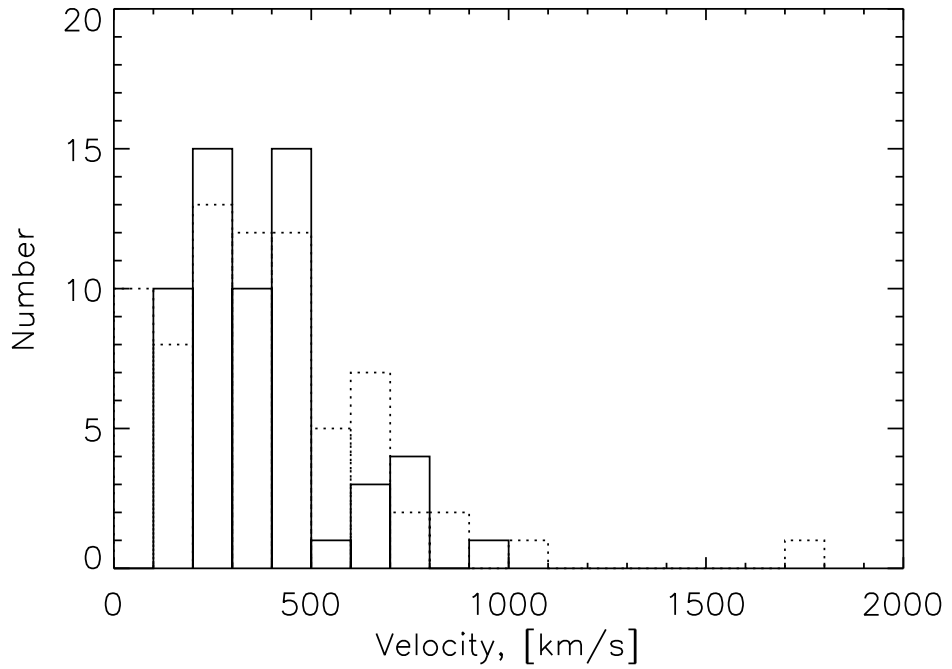

Fig. 5. Distributions of the speeds, $v^{\rm flare}$, required for the excitation of kink oscillations by a flare, in the events with (solid line) and without (dotted line) coronal type II radio bursts.

that (43%) found by Hudson & Warmuth (2004). Moreover, 16 out of these 23 type-II bursts (70%) were found to start more than one minute later than the beginning of the loop oscillations. This indicates that the shock waves are not the exciting agent of the loop oscillations. The shock waves highlighted by the type-II radio bursts are rather only a secondary phenomenon accompanying a fraction of the observed LCEs and CMEs. Indeed, all 23 type-II bursts (100%) were associated with the LCEs and 22 type-II bursts (96%) were associated with the CMEs. The lack of differences between the $v^{\rm flare}$-distributions (see Sec. 2.2) in the events with and without coronal type-II bursts (Figure 5) further confirms that the type-II bursts in the studied events (and hence the shock waves) were not the result of the flares, but the phenomenon accompanying the LCEs and CMEs (see also Gopalswamy 2006, for a comprehensive review of this issue).

It should also be noted here that in the considered cases we found that almost every event with a flare was accompanied by an LCE. However, it was not possible to establish whether the flares were triggered by LCEs, or it was the other way around. Figure 6 shows the histogram of the time differences between the beginning times of the studied LCEs and flares, and the distribution is almost symmetric with respect to zero.

3. Results

Let us briefly summarise the results of this work. We have selected 58 events of kink oscillation of EUV coronal loops, well observed by the AIA onboard the SDO during its first four years (since May of 2010 to May of 2014). 169 individual loops performing well-pronounced kink oscillations

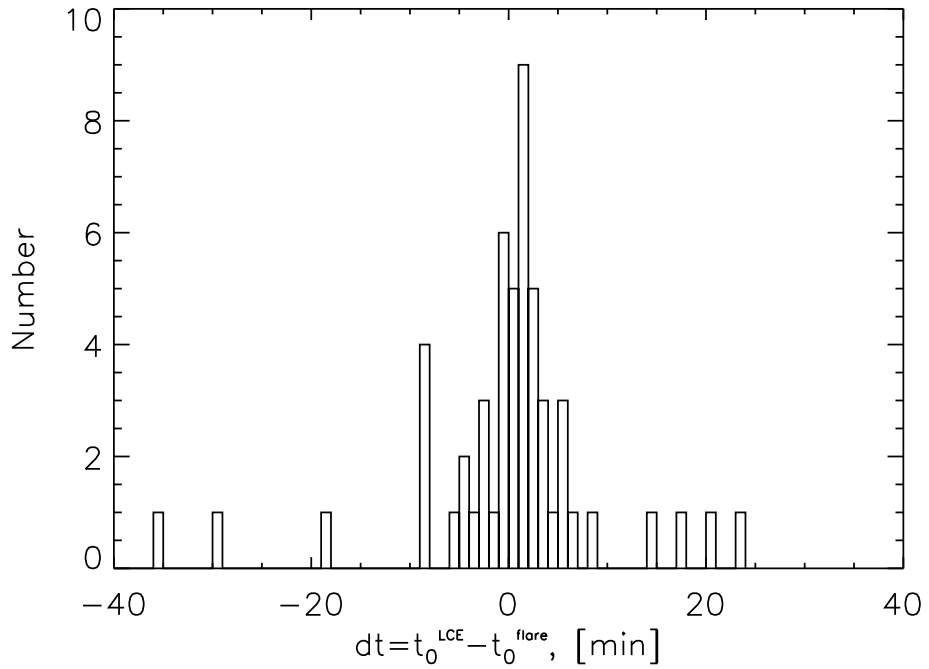

Fig. 6. Distributions of the differences between the beginning times of LCEs and flares. The time is measured in minutes. The bin size is one minute.

were selected in these events for the analysis (see Table 1). The actual number of oscillating loops in these 58 events may have been even larger than 169, since we restricted our analysis only to the consideration of the most prominent oscillating loops.

We found that 53 out of the total 58 oscillation events (i.e. 91%) were associated with flares and in five remaining events the flare sites were obviously behind the solar limb for a near the Earth observer. This **may indicate** a close relationship between flares and oscillations of coronal loops. Assuming this, we estimated the speeds of a hypothetical driver of loop oscillations caused by a nearby flare. The speed was calculated as the ratio of the distance between the flare site and and the location of the highest amplitude of the oscillation and the time between the flare **onset** and the beginning of the oscillation. This hypothetical driver is usually assumed to be a fast magnetoacoustic blast wave (e.g. Aschwanden et al. 1999; Nakariakov et al. 1999; Schrijver et al. 2002; Hudson & Warmuth 2004). These speeds were found to be lower than 500 km/s in 80% of cases. Such low speeds do not favour the blast wave mechanism, since the Alfvén speed in oscillating loops is usually higher than about $800-1,000$ km/s (e.g. Nakariakov & Ofman 2001; De Moortel & Nakariakov 2012; Stepanov et al. 2012). The Alfvén speed outside the oscillating loops – in the medium where the hypothetical driver propagates – should **not be less** than these values since the magnetic field outside the loops is **slightly** higher than inside them, while the plasma concentration inside the loop is **slightly** higher than outside it (e.g. Edwin & Roberts 1983). Thus, to be a shock wave the hypothetical driver of loop oscillations should propagate from the flare site to the oscillating loop at a speed higher than **at least** 800 **km/s**, that was not found in the majority of the cases analysed in this study. Moreover, we found that only 23 (i.e. 40%) of the loop

oscillation events were associated with coronal type-II radio bursts, that are associated with coronal blast waves. Our finding is in a good agreement with the result of Hudson & Warmuth (2004). In our opinion, as opposed to the conclusion of Hudson & Warmuth (2004), the 40% association is too low to favour the blast wave mechanism for the excitation of kink oscillations.

On the other hand, we found that 44 out of the 58 analysed oscillation events (76%) were associated with CMEs observed in the white-light emission. Even more informative fact is that 57 out of the 58 loop oscillation events (i.e. 98%) were accompanied by lower coronal eruptions or plasma ejections (LCEs) observed in the EUV band with the SDO/AIA in the parental active regions, and the remaining one was a faint event associated with a CME. Careful consideration of each loop oscillation event with the *JHelioviewer* revealed that in 55 events (95%) kink oscillations were definitely excited by the deviation of the loops from their pre-event equilibrium state by a nearby LCEs. *This is the main result of this statistical study.* Recent observational results (e.g. Harra et al. 2014, for an individual event) are consistent with this conclusion.

Two main scenarios of the excitation of kink oscillations by LCEs were thus identified as follows. The type 1 excitation was seen in 50 out of total 58 events. In the scenario of this type, kink oscillations were excited by the displacement of the loops from their equilibria by a moving (e.g. erupting and/or expanding) plasma structure such as an unstable flux rope or a system of magnetic loops. **In other five events the excitation of kink oscillations is seen to be associated with LCEs too, while there is no clear evidence of the type 1 mechanism.** In three remaining events it was difficult to unambiguously find out the driver of kink oscillations due to observational limitations. We would like to point out that there are well known other examples of kink oscillations that are not excited by the proposed mechanisms, e.g. the “harmonica event”studied by Verwichte et al. (2004).

As a byproduct of our analysis it was found that almost all the studied kink oscillation events were associated with both flares and LCEs, **which occured in the same parental active regions**. This shows a close link between these two kinds of the solar activity. However, our analysis does not allow us to conclude unambiguously whether the flares drive LCEs, or LCEs drive the flares, or both these phenomena are caused by a common reason. This conclusion is based on the finding that in about one half of the studied events the flares began prior to LCEs, and in the other half of the events the LCEs started before the flares (see Fig. 6). This problem has a long history (e.g. Sheeley et al. 1983; Dryer 1996; Jing et al. 2004; Schrijver 2009), and requires a dedicated investigation. Also, our study gives a useful catalogue (Table 1) of the kink oscillation events that can be used for follow-up studies of this interesting phenomenon.

4. Conclusions

The performed statistical analysis shows that the most probable mechanism for the excitation of kink oscillations of coronal loops is the initial displacement of the loops from their equilibria by an eruption of some unstable plasma configuration such as a flux rope or a system (arcade) of magnetic

loops, or by a plasma ejection from a flare site situated nearby, rather than a blast shock wave excited by a flare. The ascending motion of the plasma structures, or their temporary expansion, displaces coronal loops situated around them in the horizontal direction. After the passage of an ascending structures the loops return back to the previous or new equilibrium, overshoot it, and oscillate with the period prescribed by their length and the kink speed (type 1 mechanism) . This mechanism is consistent with the observed domination of the horizontally polarisation of kink oscillations.

In conclusion, we would like to emphasise that we performed a very basic and preliminary analysis of the 169 kink oscillation **loops in 58 events** summarised in Table 1. A more detailed study of this catalogue can reveal new, statistically significant properties of the oscillations.

Acknowledgements. The data used are courtesy of the SDO/AIA, STEREO/SECCHI and GOES consortia. The used SOHO LASCO CME catalogue is generated and maintained at the CDAW Data Center by NASA and The Catholic University of America in cooperation with the Naval Research Laboratory. SOHO is a project of international cooperation between ESA and NASA. The work was supported by the Marie Curie PIRSES GA-2011-295272 RadioSun Project, by the grants MK-3931.2013.2 and NSh-248.2014.2 of the President of the Russian Federation for the State Support of Young Russian PhDs and Leading Scientific Schools of the Russian Federation, by the Russian Foundation for Basic Research (project No 13-02-91165-GFEN_A) (IVZ); STFC consolidated grant ST/L000733/1, the European Research Council under the *SeismoSun* Research Project No. 321141 and the BK21 plus program through the National Research Foundation funded by the Ministry of Education of Korea (VMN).

References

Andries, J., Arregui, I., & Goossens, M. 2005, ApJ, 624, L57

Aschwanden, M. J., Fletcher, L., Schrijver, C. J., & Alexander, D. 1999, ApJ, 520, 880

Aschwanden, M. J. & Schrijver, C. J. 2011, ApJ, 736, 102

Brueckner, G. E., Howard, R. A., Koomen, M. J., et al. 1995, Sol. Phys., 162, 357

De Moortel, I. & Nakariakov, V. M. 2012, Royal Society of London Philosophical Transactions Series A, 370, 3193

Dryer, M. 1996, Sol. Phys., 169, 421

Edwin, P. M. & Roberts, B. 1983, Sol. Phys., 88, 179

Goossens, M., Van Doorsselaere, T., Soler, R., & Verth, G. 2013, ApJ, 768, 191

Gopalswamy, N. 2006, Washington DC American Geophysical Union Geophysical Monograph Series, 165, 207

Gopalswamy, N., Yashiro, S., Michalek, G., et al. 2009, Earth Moon and Planets, 104, 295

Gruszecki, M., Nakariakov, V. M., van Doorsselaere, T., & Arber, T. D. 2010, Physical Review Letters, 105, 055004

Guo, Y., Ding, M. D., Schmieder, B., et al. 2010, ApJ, 725, L38

Harra, L. K., Matthews, S. A., Long, D. M., Doschek, G. A., & De Pontieu, B. 2014, ApJ, 792, 93

Howard, R. A., Moses, J. D., Vourlidas, A., et al. 2008, Space Sci. Rev., 136, 67

Hudson, H. S. & Warmuth, A. 2004, ApJ, 614, L85

Inglis, A. R. & Nakariakov, V. M. 2009, A&A, 493, 259

Jing, J., Yurchyshyn, V. B., Yang, G., Xu, Y., & Wang, H. 2004, ApJ, 614, 1054

Khodachenko, M. L., Kislyakova, K. G., Zaqarashvili, T. V., et al. 2011, A&A, 525, A105

Khodachenko, M. L., Zaitsev, V. V., Kislyakov, A. G., & Stepanov, A. V. 2009, Space Sci. Rev., 149, 83

Kupriyanova, E. G., Melnikov, V. F., & Shibasaki, K. 2013, Sol. Phys., 284, 559

Lemen, J. R., Title, A. M., Akin, D. J., et al. 2012, Sol. Phys., 275, 17

Liu, W. & Ofman, L. 2014, Sol. Phys., 289, 3233

Liu, Y. 2008, ApJ, 679, L151

McLaughlin, J. A. & Ofman, L. 2008, ApJ, 682, 1338

Mossessian, G. & Fleishman, G. D. 2012, ApJ, 748, 140

Mueller, D., Dimitoglou, G., Caplins, B., et al. 2009, ArXiv e-prints

Nakariakov, V. M., Aschwanden, M. J., & van Doorsselaere, T. 2009, A&A, 502, 661

Nakariakov, V. M. & Ofman, L. 2001, A&A, 372, L53

Nakariakov, V. M., Ofman, L., Deluca, E. E., Roberts, B., & Davila, J. M. 1999, Science, 285, 862

Nisticò, G., Nakariakov, V. M., & Verwichte, E. 2013, A&A, 552, A57

Ofman, L. 2009, Space Sci. Rev., 149, 153

Robbrecht, E. & Berghmans, D. 2004, A&A, 425, 1097

Robbrecht, E., Berghmans, D., & Van der Linden, R. A. M. 2009, ApJ, 691, 1222

Schrijver, C. J. 2009, Advances in Space Research, 43, 739

Schrijver, C. J., Aschwanden, M. J., & Title, A. M. 2002, Sol. Phys., 206, 69

Schrijver, C. J. & Brown, D. S. 2000, ApJ, 537, L69

Sheeley, Jr., N. R., Howard, R. A., Koomen, M. J., & Michels, D. J. 1983, ApJ, 272, 349

Stepanov, A. V., Zaitsev, V. V., & Nakariakov, V. M. 2012, Physics Uspekhi, 55, A4

Török, T. & Kliem, B. 2005, ApJ, 630, L97

Török, T. & Kliem, B. 2007, Astronomische Nachrichten, 328, 743

Tothova, D., Innes, D. E., & Stenborg, G. 2011, A&A, 528, L12

Uralov, A. M. 2003, Astronomy Letters, 29, 486

Verth, G. & Erdélyi, R. 2008, A&A, 486, 1015

Verwichte, E., Nakariakov, V. M., Ofman, L., & Deluca, E. E. 2004, Sol. Phys., 223, 77

Verwichte, E., Van Doorsselaere, T., Foullon, C., & White, R. S. 2013, ApJ, 767, 16

White, R. S. & Verwichte, E. 2012, A&A, 537, A49

White, R. S., Verwichte, E., & Foullon, C. 2013, ApJ, 774, 104

Zaitsev, V. V. & Stepanov, A. V. 1982, AZh, 59, 563

Zaqarashvili, T. V., Melnik, V. N., Brazhenko, A. I., et al. 2013, A&A, 555, A55

List of Objects

Table 1. List of the coronal loop kink oscillation events detected with the AIA/SDO and their association with other phenomena in the solar atmosphere.

1	2	3	4	5	6	7	8	9	10	11	12	13	14	15	16	17	18
N	Date	t_0^{osc}	x^{osc}, y^{osc}	t_0^{flare}	t_{max}^{flare}	x^{flare}, y^{flare}	GOES	Δt^{flare}	v^{flare}	t_0^{LCE}	x^{LCE}, y^{LCE}	Δt^{LCE}	v^{LCE}	t_0^{CME}	t_0^{t2rdb}	f_0^{t2rdb}	Event
	dd/mm/yy	UT	arcsec	UT	UT	arcsec	class	s	km/s	UT	arcsec	s	km/s	UT	UT	MHz	type
1	02/08/10	04:23:12	-992, -326	04:19	04:26	-931, -269	B8.9	252	240	04:19:19	-933, -269	233	255	05:24	—	—	1
		04:24:24	-928, -377			(BEL)		314	249			295	266	(C/SA)			
2	16/10/10	19:15:24	689, -242	19:07	19:12	403, -411	M2.9	504	478	19:10:33	493, -411	291	645	20:12	19:14	*180	?
		19:16:36	762, -193					576	529			363	692				
3	03/11/10	12:14:36	-979, -379	12:07	12:21	-915, -323	C4.9	456	135	12:12:45	-919, -345	111	450	12:36	12:15	560	1
						(BEL)											
4	09/02/11	01:29:26	1048, 353	01:23	01:31	869, 316	M1.9	386	343	01:25:45	873, 310	221	591	—	—	—	1
		01:29:26	939, 444					386	274			221	490				
		01:29:26	983, 258					386	240			221	399				
5	10/02/11	04:43:48	1064, 418	04:39	04:43	884, 353	B6.0	288	482	04:37:45	890, 356	363	369	—	—	—	1
		04:43:48	1081, 366					288	497			363	382				
6	10/02/11	06:42:36	1059, 400	06:20	06:40	953, 233	C1.9	1356	106	06:37:48	1049, 435	288	92	07:36	—	—	1
														(C/L)			
7	10/02/11	06:58:12	1062, 394	06:56	06:58	923, 276	C2.1	132	1001	06:57:00	1006, 364	72	640	07:36	—	—	1
		06:58:12	1103, 369	(ZN)				132	1113			72	978	(C/L)			
		06:58:12	1102, 262					132	986			72	1410				
8	10/02/11	12:32:24	1045, 297	12:28	12:34	924, 278	C4.7	264	336	12:29:26	1010, 308	178	149	—	—	—	1
9	10/02/11	13:44:24	1061, 317	13:33	13:52	927, 282	C2.6	684	148	13:33:33	931, 288	651	148	14:12	13:50	170	1

		13:45:00	990, 408					720	145			687	141			—	
10	11/02/11	08:11:48	1100, 207	07:58	08:13	917, 317 (BEL)	B9.0	828	187	07:52:48	951, 307	1140	114	08:49	—	—	1
11	13/02/11	17:33:36	-77, -272	17:28	17:38	-85, -224	M6.6	336	105	17:33:02	-87, -231	34	900	08:49	17:35	180	1
		17:35:26	-75, -347					446	201			144	587				
		17:36:00	-274, -74					480	364			178	995				
		17:36:14	-49, -55					494	254			192	680				
12	13/02/11	20:22:36	-275, -54	20:22 (ZN)	20:24	-122, -225	B7.6	96	1733	20:13:36	-132, -229	540	303	—	—	—	2
13	13/02/11	21:27:00	-240, -55	21:27 (ZN)	21:30	-113, -227	B9.7	0	∞	21:18:00	-100, -208	540	278	—	—	—	2
14	14/02/11	02:42:24	-190, -12	02:35	02:42	-54, -209	C1.6	444	391	02:34:33	-57, -211	471	368	—	—	—	1
15	27/05/11	10:46:48	196, 347	10:27	10:53	155, 369	B3.5	1188	28	10:41:12	158, 368	336	95	—	—	—	1
		10:47:24	232, 313					1224	56			372	180				
16	11/08/11	09:58:00	1006, 217	09:34	10:23	922, 293 (BWL)	C6.2	1440	57	09:54:57	927, 273	183	384	10:36	—	—	1
		10:13:24	1027, -165					2364	144			1107	294				
17	06/09/11	22:18:38	245, 231	22:12	22:20	296, 132	X2.1	398	192	22:16:43	306, 145	115	665	23:06	22:18	680	1
		22:18:38	235, 260					398	246			115	852				
18	22/09/11	10:29:24	-1043, 382	10:29	11:01	-941, 211	X1.4	24	6015	09:59:23	-944, 207	1801	81	10:48	10:39	120	1
		10:34:12	-1114, 200					312	403			2089	59				
		10:34:12	-1068, 66					312	448			2089	65				
		10:35:24	-959, 459					384	469			2161	85				

		10:39:02	-932, 594					602	461			2379	118				
		10:55:50	-504, 529					1610	243			3387	117				
19	23/09/11	23:49:49	-973, 153	23:48	23:56	-859, 155	M1.9	109	758	23:47:57	-859, 155	112	738	00:12/	23:53	*180	1
		23:52:14	-898, 9					254	431			257	426				
		23:52:14	-945, 20					254	457			257	452				
		23:57:36	-858, -80					576	296			579	294				
20	14/11/11	07:23:48	-675, -74	07:17	07:26	-586, 97	C1.1	1368	102	07:17:48	-586, 97	360	388	07:24	—	—	1
				(ZN)										(C/SB)			
21	16/11/11	14:08:13	811, 693	14:02	14:07	893, 364	C2.4	373	659	14:04:00	889, 374	253	941	14:12	14:12	170	1
22	16/11/11	14:55:12	998, 344	14:48	15:05	915, 352	C7.9	432	140	14:43:12	919, 359	720	81	15:24	15:07	70	1
23	17/11/11	22:32:24	846, 684	22:27	22:42	873, 410	C3.2	324	616	22:26:57	873, 410	327	610	23:12	—	—	1
		22:32:24	877, 731			(BWL)		324	718			327	712				
		22:32:48	745, 774					348	804			351	797				
24	18/11/11	07:34:38	-683, -588	07:32	07:37	-646, -452	C1.5	158	647	07:29:12	-645, -455	326	308	07:54	—	—	1
		07:36:00	-882, -573					240	801			408	470	(C/SB)			
		07:36:00	-831, -616					240	747			408	437				
25	22/12/11	01:59:12	346, -171	01:56	02:08	293, -265	C5.4	192	407	01:47:24	304, -229	708	73	02:54	02:04	150	1
		02:02:48	257, -336					408	141			924	92	(C/SB)			
26	16/01/12	00:08:12	1051, 92	—	—	—	—	—	—	00:06:31	1013, 65	101	335	00:54	00:40	100	1
		00:10:00	1098, 34			(BWL)		—	—			209	314	(C/SB)			
27	09/04/12	01:15:12	1043, 86	01:11	01:22	925, 236	C2.6	252	138	01:13:24	930, 208	108	1281	02:00	—	—	1

		01:15:12	1065, 93					252	145			108	1343				
		01:15:12	1015, 68					252	138			108	1279				
		01:20:00	1033, -211					540	33			396	842				
28	30/04/12	07:04:00	1156, -245	06:56	07:38	896, -311	C3.9	480	405	06:55:45	897, -297	495	245	07:48	07:27	100	1
29	08/05/12	13:06:38	-635, 353	13:02	13:08	-662, 263	M1.4	278	245	13:05:24	-680, 266	74	960	—	—	—	2/3
		13:06:38	-654, 391					278	334			74	1251				
30	17/05/12	01:30:14	1052, 186	01:25	01:47	940, 128	M5.1	314	291	01:16:33	1060, 100	821	76	01:48	01:32	*180	1
		01:30:14	1048, 158					314	259			821	52				
		01:33:50	1023, -350					530	664			1037	316				
		01:33:50	1052, 402					530	405			1037	211				
		01:35:01	785, -121					601	354			1107	231				
31	26/05/12	20:38:00	964, 368	—	—	—	—	—	—	20:35:12	945, 351	168	110	20:57	20:47	120	1
		20:38:00	974, 329			(BWL)		—	—			168	157				
		20:44:00	1185, 307					—	—			528	335				
		20:44:36	1183, 53					—	—			564	490				
		20:43:48	1045, -145					—	—			516	711				
		20:45:12	1066, -251					—	—			600	742				
32	30/05/12	09:00:24	-1004, -354	08:36	08:48	-948, -317	C1.1	1464	33	08:59:09	-953, -322	75	582	09:54	—	—	1
		09:00:24	-1004, -369	(ZN)		(BEL)		1464	38			75	670	(C/SB)			
		09:00:24	-998, -388					1464	43			75	772				
		09:00:24	-985, -405					1464	47			75	860				
33	06/07/12	23:06:37	886, -71	23:01	23:08	805, -253	X1.1	337	429	23:02:13	817, -219	264	448	23:24	23:09	180	1

		23:07:02	897, -621					362	760			289	1028				
		23:07:26	792, -620					386	690			313	931				
		23:10:00	1000, -63					540	366			467	373				
34	07/08/12	00:59:23	-1058, -131	00:55	00:58	-904, -238	B8.9	263	517	00:56:59	-905, -223	144	899	01:48	—	—	1
35	07/08/12	01:35:24	-1059, -131	01:31	01:34	-915, -207	C1.0	264	447	01:32:23	-918, -200	181	629	01:48	—	—	1
		01:37:11	-1077, -179			-915, -207		371	321			288	404				
36	07/08/12	03:02:59	-1063, -129	03:08	03:17	-893, -253	C2.0	-301	—	02:49:47	-906, -208	792	161	04:00	—	—	2
37	15/10/12	21:54:35	-1102, 12	21:52	21:55	-913, 137	B7.3	155	1060	21:49:47	-917, 136	288	561	—	—	—	2
		21:58:11	-1114, -19	(ZN)				371	497			504	361				
38	19/10/12	19:02:47	-1049, -163	—	—	—	—	—	—	18:59:11	-962, -139	216	303	—	—	—	1
		19:03:23	-1068, -182			(BEL)		—	—			252	329				
		19:03:59	-1113, -181					—	—			288	395				
39	19/10/12	21:00:35	-1091, -168	20:46	20:52	-940, -231	C3.6	875	136	20:45:35	-947, -223	900	124	21:24	—	—	1
		21:00:35	-1103, -192			(BEL)		875	139			900	128				
		21:00:35	-1108, -114					875	170			900	157				
40	20/10/12	18:08:35	-1017, -233	18:05	18:14	-945, -204	M9.1	215	262	18:04:32	-949, -204	243	221	18:36	18:15	*180	1
		18:09:11	-1043, -220					251	287			269	257				
		18:10:23	-1021, -311					323	295			351	266				
		18:10:59	-1105, -140					359	348			387	316				
		18:10:59	-1073, -96					359	338			387	308				
		18:10:59	-1043, -103					359	284			387	258				

		18:11:35	-1084, -382					395	415			423	383				
		18:13:24	-972, -424					504	319			532	301				
41	21/11/12	15:21:35	-206, -15	15:10	15:30	-101, 73	M3.5	695	143	15:18:13	-122, 39	202	358	16:00	15:31	130	1
		15:21:35	-245, -48					695	196			202	541				
		15:25:11	-264, -141					911	214			418	398				
		15:25:49	-425, 125					949	238			456	501				
42	05/01/13	09:29:47	-961, 413	09:26	09:31	-906, 351	M1.7	227	265	09:28:56	-938, 373	51	656	09:24	—	—	1
		09:30:23	-1052, 453					263	491			87	1161				
		09:30:59	-1053, 489					299	489			123	963				
		09:31:35	-1008, 529					335	444			159	780				
		09:31:35	-1064, 584					335	609			159	1121				
		09:31:35	-1099, 353					335	418			159	740				
		09:32:11	-1123, 324					371	427			195	712				
43	07/01/13	06:38:11	865, 607	06:35	06:39	791, 505	C1.0	191	478	06:35:59	795, 517	132	626	—	—	—	1
		06:38:11	812, 673					191	643			132	862				
		06:38:11	900, 650					191	689			132	931				
		06:41:11	942, 733					371	534			312	607				
44	07/01/13	08:47:59	860, 581	08:44	08:52	792, 509	C3.1	239	300	08:47:11	802, 511	48	1350	—	—	—	1
		08:48:37	799, 611					277	268			86	827				
		08:48:37	816, 659					277	398			86	1236				
		08:49:11	900, 640					311	396			120	969				
		08:49:11	932, 657					311	475			120	1172				
45	17/02/13	15:48:23	-377, 380	15:45	15:50	-344, 412	M1.9	203	164	15:46:32	-356, 319	111	421	—	15:48	400	1

46	24/05/13	18:54:47	-1041, -281	18:51	18:53	-949, -172	B6.6	227	456	18:52:23	-960, -188	144	621	20:24	—	—	2
		18:55:23	-1130, -345					263	690			180	932	(C/S-A)			
47	27/05/13	01:57:47	322, -147	01:49	02:11	295, -254	B8.1	527	152	01:54:11	315, -239	216	310	02:54	—	—	1
		01:57:47	368, -106					527	227			216	481	(C/S-A)			
48	18/07/13	17:56:11	-1134, -35	17:56	18:23	-914, -229	C2.3	11	19332	≲17:20:00	-934, -240	2171	96	18:24	—	—	1
		17:56:47	-1110, 12					47	4792			2207	101	(C/L)			
		17:57:23	-1165, 45					83	3246			2243	119				
		17:57:59	-1150, 76					119	2350			2279	122				
49	11/10/13	07:08:59	-1063, 338	07:01	07:24	-901, 378	M1.6	479	253	07:07:47	-1033, 271	72	739	07:24	07:11	250	1
		07:12:23	-1071, 100			(BEL)		683	346			276	460				
		07:14:59	-1016, -40					839	375			432	523				
		07:17:35	-1071, -224					995	456			588	612				
		07:18:35	-1078, -280					1055	494			648	619				
50	19/11/13	10:19:59	1056, -221	10:14	10:26	874, -238	X1.0	359	369	10:15:32	888, -251	267	463	10:36	10:22	400	1
		10:19:59	1064, -181					359	401			267	514				
		10:19:59	921, -73					359	346			267	492				
		10:23:35	831, -468					575	295			483	337				
51	19/12/13	23:10:11	-1013, -305	23:06	23:26	-925, -252	M3.5	251	297	23:08:56	-935, -247	75	940	23:48	—	—	1
		23:14:59	-1102, -217					539	243			363	339	(C/L)			
		23:15:11	-1108, -142					551	281			375	391				
		23:15:49	-1070, -432					589	285			413	402				
		23:15:49	-1023, -516					589	347			413	497				

		23:17:00	-1105, 5					660	345			484	455				
52	04/01/14	15:33:11	-667, 98	15:33	15:47	-586, -6	C9.4	11	8688	15:28:23	-629, 52	288	150	—	—	—	1
53	06/01/14	07:44:23	1069, -384	07:42	07:45	924, -259	C2.1	143	971	07:42:20	931, -254	123	1117	08:00	07:45	*180	1
		07:45:35	1108, -159	(ZN)				215	706			195	747	(C/L)			
54	10/02/14	21:00:35	1161, 49	21:00	21:03	—	C1.2	35	—	20:57:44	1032, 61	171	549	21:24	—	—	1
		21:00:35	1059, 22	(ZN)		(BWL)		35	—			171	201	(C/S-A)			
		21:00:35	1113, 30					35	—			171	368				
		21:00:35	1108, 243					35	—			171	836				
		21:03:35	1184, 103					215	—			351	326				
55	10/02/14	22:48:47	1103, 266	—	—	—	—	—	—	—	—	—	—	23:24	—	—	—
		22:48:47	1112, 238			(BWL)		—	—			—	—	(C/L)			
		22:48:47	1160, 192					—	—			—	—				
		22:48:47	1187, 146					—	—			—	—				
56	11/02/14	13:26:35	1090, 155	—	—	—	—	—	—	13:25:44	1017, 109	51	1227	14:00	13:27	650	1
		13:27:11	1068, 209			(BWL)		—	—			87	935	(C/L)			
		13:27:47	1006, -11					—	—			123	710				
		13:28:23	1098, 261					—	—			159	785				
		13:28:59	1133, -5					—	—			195	605				
		13:28:59	1093, -35					—	—			195	605				
		13:30:23	1078, 393					—	—			279	755				
		13:30:23	1036, 399					—	—			279	755				
		13:30:59	1042, 457					—	—			315	803				
57	24/02/14	11:05:35	-1010, -157	11:03	11:17	-951, -171	M1.2	155	284	$\lesssim$11:00:00	-960, -152	335	109	11:36	—	—	1

	11:06:11	-1049, -198				155	386			371	196	(C/L)				
	11:10:23	-1149, -309				443	395			623	286					
58	16/04/14	19:57:35	-329, -288	19:54	19:59	-151, -147	M1.0	215	766	19:55:47	-141, -142	108	1598	20:00	19:58	*420	1
														(C/L)			